High-Speed Spiking and Bursting Oscillations in a Long-Delayed Broadband Optoelectronic Oscillator

Bruno Romeira, *Member, IEEE*, Fanqi Kong, *Student Member, IEEE*, José M. L. Figueiredo, *Member, IEEE*, Julien Javaloyes, *Member, IEEE*, and Jianping Yao, *Fellow, IEEE, Fellow, OSA*

***Abstract*—We investigate the generation of high-speed spiking and bursting signals in a long time-delayed broadband optoelectronic oscillator (OEO). The OEO is configured in a delayed feedback loop employing a long optical fiber delay line and other elements including a tunable laser, a phase modulator (PM) and a linearly chirped fiber Bragg grating (LCFBG), a photodetector, and an electrical amplifier. The joint operation of the PM and the LCFBG forms an ultrawideband microwave photonic filter (MFP). Taking advantage of the multiple time scales arising from the MPF and the long optical fiber delay line, we are able to generate subnanosecond neuron-like spiking and bursting signals that emulate the response found to be the primary mode of electrical firing in biological neurons. Since our OEO can operate at a much higher speed and can be controlled using both time-delayed feedback employing low-loss optical fiber and electrical/optical injection locking techniques, it has interest in emerging photonics applications such as neuromorphic information processing and reservoir computing tasks.**

***Index Terms*—Delayed systems, fiber bragg grating, microwave generation, microwave photonics, neuromorphic spiking, optoelectronic oscillator, signal processing.**

I. Introduction

SPIKING and bursting oscillations are an interesting phenomenon attracting continued attention over the years. They are produced by excitable systems as diverse as cells responsible for vital neurological rhythmicity [1], mixed-mode oscillations of chemical systems [2], or engineering systems including lasers [3]–[6]. Spiking signal processing where information is encoded as events in time has been recently proposed in neuromorphic systems employing semiconductor microstructures [7] and excitable lasers [8] to implement optical reservoir computing that exploits the high-speed and low crosstalk available in photonic interconnects. Therefore, the ability to produce short optical pulses, with correspondingly large bandwidths, in photonics is very useful for applications such as clock recovery, pulse reshaping, and artificial neural networks that take advantage of spiking information processing [8], [9]. However, slow speed operation, complexity, and costly fabrication make most of the proposed laser schemes for spiking signal generation far from the requirements of high-speed information processing systems.

Optoelectronic oscillators (OEOs) [10], [11] are hybrid devices in which the signal propagates alternately in the optical and in electronic domains. OEOs offer significant advantages for high-speed signal processing applications because they combine the robustness of electronics with the wide bandwidth of optics. In addition, the ability to easily control the OEO operating conditions based on both time-delayed feedback employing low-loss optical fibers, and electrical/optical injection locking techniques adds extra flexibility.

Recently, a considerable number of OEOs [10]–[18] has been explored for the generation of fast continuous-wave (CW) and self-pulsating signals by taking advantage of the low loss of an optical fiber, which is utilized as a long delay line to increase the quality factor of an OEO. On the one hand, an OEO can generate a CW microwave signal at a frequency up to tens of gigahertz with an extremely low phase noise [10]–[13]. On the other hand, the generation of ultra-low jitter optical pulses has been also demonstrated using a coupled-OEO [14], or time-lens soliton-assisted compression of sinusoidally modulated pulses [15], or using a self-oscillating heterojunction bipolar phototransistor [16], or employing an electro-absorption modulator [17], or using passive mode-locking [18] in an OEO. Furthermore, OEO systems have also shown potential for the generation of rich and complex phenomena that include chaotic signals [19], breathers [20], [21], excitable spikes [22], and multipulse dynamics [21].

In most of the aforementioned OEO configurations [15]–[18], [22], the efforts are focused mainly in the generation of periodic and fast- self-pulsating behavior. The achieved pulsed regimes are also strongly dependent on the radio-frequency (RF) components, namely the electrical filter, that are used to tailor the OEO characteristics. In this work, we present a comprehensive investigation on the dynamical regimes occurring in a long-delayed broadband OEO including the generation of high-speed

Manuscript received September 21, 2014; revised November 12, 2014; accepted November 26, 2014. Date of publication December 1, 2014; date of current version January 26, 2015. This work was supported in part by the Natural Sciences and Engineering Research Council of Canada (NSERC), by FCT Portugal for a Postdoctoral Fellowship under Grant SFRH/BPD/84466/2012, and by the Ramón y Cajal fellowship.

B. Romeira is with the Microwave Photonics Research Laboratory, School of Electrical Engineering and Computer Science, University of Ottawa, Ottawa, ON K1N 6N5, Canada, and also with the Center for Electronics, Optoelectronics and Telecommunications, Department of Physics, University of the Algarve, 8005-139 Faro, Portugal (e-mail: bmromeira@ualg.pt).

F. Kong and J. Yao are with the Microwave Photonics Research Laboratory, School of Electrical Engineering and Computer Science, University of Ottawa, Ottawa, ON K1N 6N5, Canada (e-mail: jpyao@eecs.uottawa.ca).

J. M. L. Figueiredo is with the Center for Electronics, Optoelectronics and Telecommunications, Department of Physics, University of the Algarve, 8005-139 Faro, Portugal.

J. Javaloyes is with the Department de Fisica, Universitat de les Illes Baleares, E-07122 Palma, Spain.

Color versions of one or more of the figures in this paper are available online at http://ieeexplore.ieee.org.

Digital Object Identifier 10.1109/JLT.2014.2376775

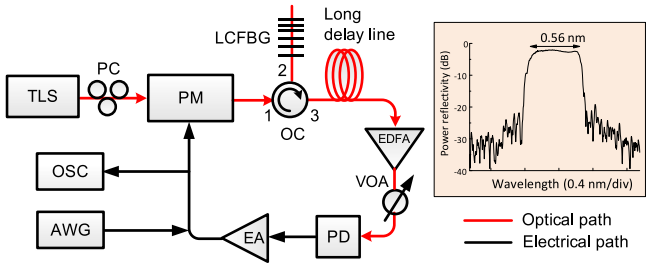

Fig. 1. Schematic of the long-delayed broadband OEO. The LCFBG power reflectivity is shown as an inset.

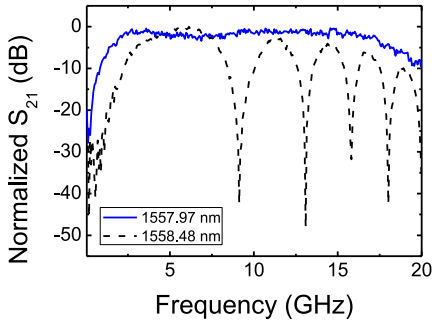

Fig. 2. The broadband spectral response of the OEO open loop.

randomly neuromorphic spiking and bursting signals. The OEO combines a phase modulator (PM) and a linearly chirped fiber Bragg grating (LCFBG) forming an ultra-wideband microwave photonic filter (MPF) which allows to tailor in the optical domain the broad bandpass characteristics of the OEO. Recently, taking advantage of this experimental setup, we have demonstrated the capability of the broadband LCFBG-based OEO to achieve complex signal generation including chaos and breather oscillations [20]. Here, we investigate the generation of sub-nanosecond spiking-bursting signals that resemble the spiking phenomena found to be the primary mode of electrical firing behavior in biological neurons [23]. We explore the generation of fast neuron-like spiking phenomena taking advantage of the multiple time scales arising from the MPF and the long optical fiber delay line in the OEO.

The complex spiking patterns reported here are ubiquitous phenomena revealing co-existing alternating fast oscillations and slow bursting signals that can be controlled by the parameters of the OEO including the gain, fiber length, and external injection. Considering that similar pattern formation has been found to regulate local synaptic activity observed in large neuronal networks [24], the investigation of these signals in a delayed-feedback OEO reveals great potential for complex information processing tasks in microwave-photonics systems such as coding and memory formation for neuromorphic information processing and reservoir computing applications.

II. Principle

The block diagram of the long-delayed broadband OEO is shown in Fig. 1. It consists of a tunable laser source (TLS) (1440–1640 nm) providing up to 6.3 mW output optical power, a polarization controller (PC), a broadband PM with a modulation bandwidth of 20 GHz, an LCFBG, an optical circulator (OC), an optical fiber delay line, an erbium-doped fiber amplifier (EDFA), a variable optical attenuator (VOA), a photodetector (20 GHz) with a responsivity of 0.85 A/W at 1550 nm, two cascaded electrical amplifiers (EAs), and an arbitrary waveform generator (AWG) that provides electrical injection of a control signal. The LCFBG has a 3-dB bandwidth of 0.56 nm, shown as an inset in Fig. 1, a dispersion value of 1457 ps/nm, and a peak power reflectivity of 95%. The electrical amplification is provided by the two cascaded EAs (bandwidth of 30 kHz to 10 GHz) with an electrical gain up to 55 dB.

A CW light wave from the TLS is sent to the PM. The phase-modulated signal from the PM is sent to the LCFBG through the OC and then time delayed using a long single mode fiber. After amplification by the EDFA, the optical signal is converted to an electrical signal at the PD. At last, the electrical signal is amplified by the EA and fed back to the PM, to close the OEO loop. The VOA is used to tune the optical attenuation and therefore adjusting the total gain of the feedback loop. The operating conditions of the OEO can be further controlled by means of external injection of an electrical signal here generated by an AWG. The signal produced by the OEO is monitored in the electrical domain using a fast real-time digital oscilloscope (Agilent DSA-X 93204A Infiniium, 32 GHz).

In terms of frequency response, the broadband OEO can be configured to operate in two regimes, depending on the wavelength of the CW light wave. When the wavelength is located within the LCFBG reflection window, the two first-order sidebands of the phase-modulated signal will first be in phase, then anti-phase, and then in phase again because of the group velocity dispersion of the LCFBG, that corresponds to the various resonance peaks in the frequency response shown in Fig. 2 (dashed line). When the wavelength is located in one of the LCFBG slopes, a destructive interference will never occur since one of the sidebands is suppressed. Therefore, if the wavelength of the optical carrier is properly selected to make it located at one of the slopes, an OEO with a broadband MPF is realized. The frequency response of the LCFBG when the wavelength is located on the left upward slope ($\lambda = 1557.97$ nm) is shown as a solid line in Fig. 2. As can be seen the frequency response in this case exhibits a flat response with only one passband instead of multiple resonance peaks. The bandwidth of our LCFBG is around 0.56 nm (the LCFBG can be designed with a larger reflection window that can go above 1 nm). This corresponds to an equivalent frequency bandwidth of more than 100 GHz which is much higher than the bandwidth of an electronic filter usually employed in an OEO, which makes this regime of operation particularly suitable for the generation and processing of ultra-wideband signals.

In this work, we explore specifically the regime of operation where the MPF and the frequency response of the electronic and optoelectronic components induce a broad bandpass filtering property with a flat response with only one passband for the generation of spiking and bursting oscillations. The OEO

can be considered as an experimental realization of a modified Ikeda time-delayed equation [25] and it is modeled employing a bandpass nonlinear dynamical delay differential equation (DDE) [21]. In order to capture the dynamics observed experimentally, specifically the fact that in our OEO the MPF and the frequency response of the electronic and optoelectronic components induces broad bandpass filtering, we assume that the frequency filtering process can be modeled in the time domain by an integro-differential operator characterized by both high- and low-cutoff frequencies [20], [21]. The OEO is described by an integro-differential equation that provides a phenomenological description of our system, so that the dynamics of the RF voltage at the input of the PM in its dimensionless form reads as [20],

$$\begin{aligned} x' &= -\varepsilon y - x + \beta \sin\left[x(t-T) + \chi\xi(t) + \phi_0\right] \\ y' &= x \end{aligned} \tag{1}$$

where the dimensionless dependent variable $x(t) = \pi V(t)/V_{\pi \mathrm{RF}}$ is proportional to the RF voltage in the electronic feedback driving the PM, $V_{\pi \mathrm{RF}}$ is the half-wave voltage of the PM, $\varepsilon = \tau/\theta$ is the ratio between the low and high cut-off frequencies, ϕ_0 is a constant offset phase, and T the dimensionless delay time. The overall feedback gain is given by $\beta = \pi\gamma K^2 G_0 \Re P_0 / V_{\pi \mathrm{RF}}$, where γ accounts for the optical power losses; $K$is the slope steepness factor of the LCFBG, $\Re$ is the responsivity of the PD, P_0 is the optical intensity input, and G_0 stands for the amplifier gain. A detailed description of the model and physical parameters can be found in [20]. There are several effects that contribute to the noise in our OEO: thermal noise in the amplifiers, shot noise in the PD, the intensity noise of the TLS, and the spontaneous emission noise of the EDFA. Since the majority of these fluctuations are characterized by a Gaussian random process, we have chosen to model the stochastic processes in our OEO as an effective delta-correlated Gaussian white noise with zero mean $\chi\xi(t)$ [26], corresponding to a stochastic voltage source that takes into account all the noise contributions, where the parameter χ is the dimensionless variance of the distribution that is equal to unity and denotes the noise strength. In this method, the stochastic noise contribution is added after the deterministic step by simply using the Euler method [26] and scaling the noise strength as $\sqrt{h}$, where *h* is the simulation time step. The effect of noise in the OEO dynamics can be observed after only a few delayed feedback round-trips providing less time consuming numerical simulations when compared with other choices for the noise modeling, namely the additive noise method reported in [27], where the influence of noise in the OEO dynamics is strongly dependent on the number of simulated time round-trips.

III. Results

Spiking and bursting oscillations are common patterns of electrical activity in excitable cells such as neurons [23], [24], [28] and many endocrine cells [29], [30]. Bursting activity is characterized by alternation between periods of spiking and periods of rest, and is driven by slow variations in one or more slowly changing variables, such as the intracellular calcium concentration. Bursting oscillations in excitable systems reflect multi-timescale dynamics [31]–[33]. Our broadband OEO is a special case of a slow-fast system providing multiple time scales arising from the MPF and the long optical fiber delay lines employed in the experiments. There are three different time-scales in our OEO: the microwave carrier frequency in the gigahertz range, the filter low cutoff frequency in the MHz range, and the free spectral range (FSR) that spans from the kilohertz range up to the MHz range, depending on the length of the delay line.

In what follows, we investigate the spiking and bursting dynamical regimes observed in the broadband OEO when the delay time, τ_d, is much larger than the other typical time scales of the system.

A. Random Spiking-Bursting Signals

Typically, excitable systems are characterized by a stable steady state that may be forced to spike by relatively small perturbations above some threshold for parameter regimes where a stable fixed point is close to a bifurcation in which oscillations are created (see [34], [35] and references therein). They involve multiple time-scale dynamics. Low-dimensional systems normally display such behavior near Hopf bifurcations, when a fixed point becomes unstable in favor of self-sustained stable oscillations. However, considerably richer scenarios are possible in higher-dimensional systems such as the case of delayed feedback systems, particularly for large time delay systems as the one reported here.

In the following, we investigate the generation of spiking-bursting signals by varying the feedback gain and optical fiber time delay conditions of the system. Specifically, we employ in the experiment an optical fiber delay line with three different lengths or time delays $\tau_d : \tau_{d1} = 0.33$ μs, $\tau_{d2} = 4.40$ μs and $\tau_{d3} = 6.38$ μs, which are measured according to the FSR of the OEO. For sufficient long optical fiber delays, the FSR is given approximately by:

$$\mathrm{FSR} \cong \frac{c}{n_{\mathrm{eff}} L} \tag{2}$$

where n_{eff} is the optical fiber effective refractive index, *c* is the velocity of light in vacuum, and *L* the length of the fiber.

In the experiment, the wavelength of the light wave is selected to be located at the left slope of the LCFBG reflection window ($\lambda = 1558.093$ nm). The TLS optical power is set at 5.7 mW and the maximum power received by the PD is $P_0 \sim 1$ mW. The VOA is used to control the level of optical power, P_0, received by the PD, and thus the gain conditions of the OEO. For $P_0 > 0.12$ mW and a time delay of $\tau_{d1} = 0.33$ μs, the OEO starts to oscillate at a frequency of $\sim$1.25 GHz. Fig. 3 shows the experimentally generated temporal waveforms for long time traces (a few time delays, left), and short time traces (tens of nanosecond, right), displaying different signals as a function of the feedback gain and the time delay. When the optical power is increased, at $P_0 = 0.36$ mW, the signals generated exhibit two time scales, as shown in Fig. 3(a) and (b), one appearing at the fast 1.25 GHz oscillation corresponding to an inter-burst time scale of 0.8 ns, the fastest component of the signal, and the other to 0.33 μs corresponding to the slow envelope modulation

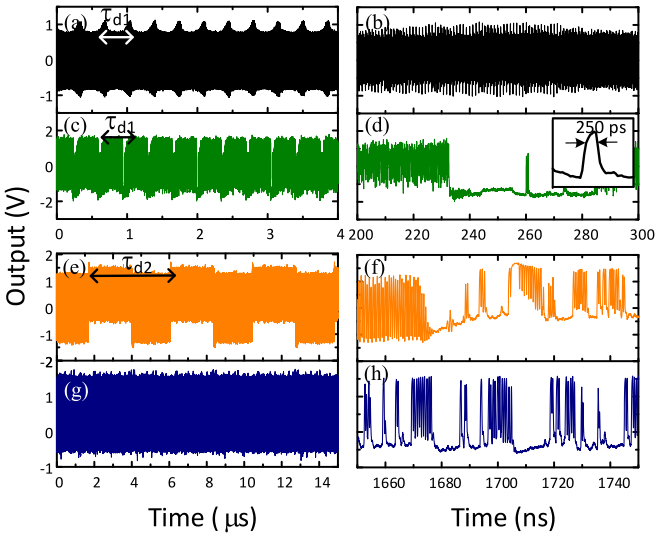

Fig. 3. Experimental time traces of the oscillating (nominal frequency ∼1.25 GHz) and spiking signals as a function of the optical power and time delay: (a), (b) oscillations ($P_0 = 0.36$ mW and $\tau_{d1} = 0.33$ μs); (c), (d) breathers and spikes ($P_0 = 0.43$ mW and $\tau_{d1} = 0.3$ μs); (e), (f) oscillations and spikes ($P_0 = 0.57$ mW and $\tau_{d2} = 4.4$ μs); (g), (h) spiking-bursting signals ($P_0 = 0.73$ mW and $\tau_{d3} = 6.38$ μs).

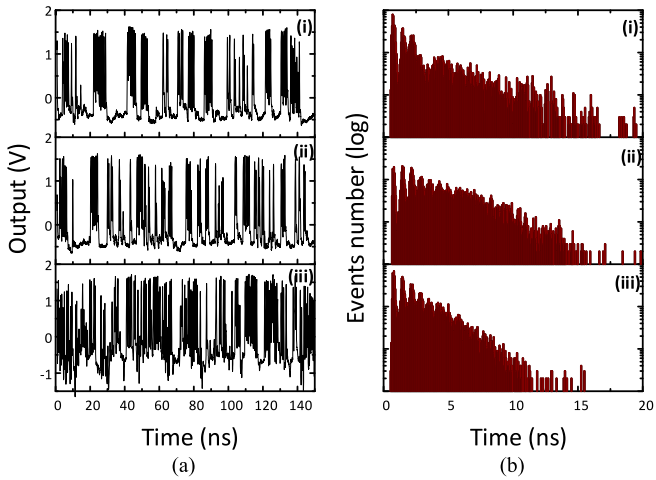

Fig. 4. (a) Spiking-bursting signals in the time domain using a time delay of 6.38 μs as a function of the optical power: (i) $P_0 = 0.73$ mW (ii) $P_0 = 0.77$ mW (iii) $P_0 = 0.96$ mW. (b) The corresponding ISI histograms with a bin size of 50 ps.

around 3 MHz, which is a consequence of the delay influence being greater. This type of Neimark–Sacker bifurcation is a characteristic of a system employing a bandpass filter [20], [36] where a secondary Hopf bifurcation appears with a frequency that is not half of the fundamental as it would be for the period doubling scenario but it is related with the time delay. This is a characteristic of a route to chaos via quasi periodicity and of the so called Ruelle–Takens mechanism.

Further increasing the feedback gain, the OEO can sustain chaotic breather signals, as shown in Fig. 3(c), before reaching a fully developed chaotic signal. Chaotic breathers are characterized by nanosecond chaotic oscillations breathing periodically at a significantly lower time-scale and have been investigated recently [20]. In a close view of the signals, shown in Fig. 3(d), we observe that the breathers also show signatures of spiking behavior before reaching a chaotic state [Fig. 3(d) shows a sequence of two isolated spikes between self-sustained oscillations]. The duration, profile, and amplitude of the generated spikes are identical and the pulse width is mainly determined by the cut-off frequency of the broadband OEO. The typical measured full-width half-maximum is 250 ps, as shown in the inset of Fig. 3(d), which is limited by the 50 ps sampling resolution of the oscilloscope.

The spikes with identical shape and amplitude are similar to the spiking phenomena found in the primary mode of an electrical firing behavior in biological neurons which has been well described within a framework of the methods of qualitative theory of slow-fast systems. A comprehensive review was provided in [37], where some transitions between tonic spiking and bursting are associated with the chaotic behavior. Since our broadband OEO is a special case of a slow-fast system providing multiple time scales arising from the MPF and the optical fiber delay line, it is expected that these dynamical regimes can arise when we tune the OEO operating conditions near a chaotic regime. Furthermore, spiking phenomena has been reported in other OEOs when the system approaches other bifurcation regions, particularly through an Andronov–Hopf bifurcation, as discussed in [22], [35]. Although this is not analyzed in this work, we have experimentally observed spiking excitation in the transition from a steady-state to an oscillating condition, that is, through an Andronov–Hopf bifurcation which is also confirmed by our preliminary modeling results. Currently underway is a more detailed study on the spiking behavior in this region which could be interesting from the experimental point of view given the small gain conditions required to achieve this regime.

We observe that the regularity of spikes increases with the length of the optical fiber delay line, as shown in Fig. 3(e) and (f). We also observe that instead of firing individual spikes, the OEO exhibits a multi-pulsing bursting behavior where the duration of bursting grows as the gain control parameter is increased, while the inter-burst interval remains nearly constant (close to the period of the self-oscillations). This scenario of transition from tonic spiking into bursting follows a Neimark–Sacker type route to chaos since the bursting behavior is not regular but chaotic, similarly as the first multi-pulsing phenomena reported in [21]. Fig. 3(g) and (h) shows fully sustained spiking-bursting as we move away from the Neimark-Sacker bifurcation into a chaotic regime and employing a long time delay of 6.38 μs where only the spiking signals remain and the oscillations are absent.

In Fig. 4(a) we show spiking-bursting signals for various gain conditions exhibiting similar spiking regimes as shown in Fig. 3(h). To obtain further information about the time traces displayed in Fig. 4(a), we investigate the probability distribution of the interspike intervals (ISIs). From the analysis of ISI statistics, shown as histograms in Fig. 4(b), we see a typical exponential distribution of a Kramer's escape process typical of random processes with a hard boundary on the left. This allows estimating

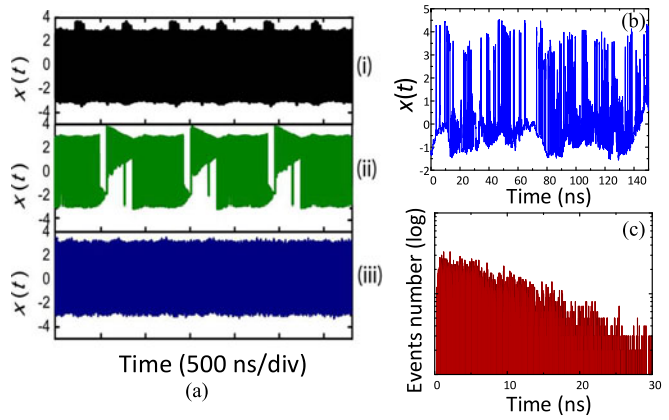

Fig. 5. (a) Numerical simulations of $x(t)$ output showing the evolution of the dynamics as a function of the time delay: (i) 0.33 μs; (ii) 1 μs; (iii) 6 μs. (b) Numerical simulations of $x(t)$ output employing $\beta = 2.5$ and a time delay of 6 μs, showing the spiked signals in the time domain, and (c) the corresponding ISI histograms with a bin size of 15 ps.

the OEO response time to be 450 ± 50 ps which is close to the typical OEO self-sustained oscillation period ($\sim$800 ps).

The ISI histograms, shown in Fig. 4(b), also reveal that the bursts manifest themselves in the histograms as a peaked structure at n/T_l where $T_l = 450$ ps corresponds to the response time. This means that in this bursting regime, if we have fired spike at T_1, it is likely to be followed by another one at $T_2 = T_1 + T_l$. From the comparison between Fig. 4(b)-(i)–(b)-(iii) we observe that the slope of the tail of the distribution decreases with higher optical power as a result of the increasing firing of multi-spikes as we move close to a chaotic regime. In the literature, this type of bursting phenomena is referred in many systems to as chaotic itinerancy [38], that is, a dynamic regime in which a system switches back and forth between ordered dynamical regimes.

The dynamics of the spiking behavior is further analyzed by numerical simulations for the phenomenological DDE system given in (1). The results are shown in Fig. 5, which confirm that self-pulsating signals similar to the signals observed experimentally can be sustained. The DDE system is integrated with a time step of $h = 0.1$, which corresponds to a $dt = 1.5$ ps, over N round trips in the optoelectronic feedback loop. At each round trip the signal is propagated in the OEO and computed according to the fourth order Runge–Kutta algorithm. In order to avoid very long time simulations and large memory requirements, we have chosen a time sampling of 10, i.e., 1 point every 10 is sampled.

Fig. 5(a) presents the evolution of the dynamics for increasing values of delay showing the splitting of the OEO time scales (i), and a transition from breather oscillations (ii) to spiking-bursting oscillations (iii), as demonstrated experimentally in Fig. 3. Fig. 5(b) and (c) displays the results of the numerical simulations in the time domain and the corresponding ISI statistics, respectively, for a region of spiking behavior by choosing a large delay and moderate gain feedback conditions. In the numerical simulations we employ a time delay of 6 μs, 1.5×10^{-3} to account for the bandpass filtering effect, $\phi_0 = \pi$, and $\chi = 10$. We have considered a total simulation time of about 1.5 ms providing a sufficient large number of delay loops to fully observe the underlying dynamics induced by the delayed feedback. The simulation results in Fig. 5(b) confirm the dynamics observed experimentally, which show the random spiked signals in the time domain. From the analysis of ISI statistics, shown in Fig. 5(b), we see a typical exponential distribution of a Kramer's escape process typical of random processes with a hard boundary on the left, showing a response time of 300 ± 15 ps, which is similar to the typical response observed experimentally in our OEO.

The simulation results indicate that, under the operating conditions reported here, our experimental system is a strongly noise driven system which corresponds to what we would expect considering the noise sources of our system, namely the thermal noise of the two EAs. However, it is also important to note that in our model the stochastic noise contribution is added after the deterministic step and the noise strength scales as $\sqrt{h}$, where h is the simulation time step (see Section II). Therefore, in order to take into account the relation between χ and the physical noise intensity values we must also pay attention to the time scaling and the simulation time step. Since in a long-delayed feedback OEO a larger time step is typically employed in the simulations to avoid time consuming simulations and save computing memory storage, this results in a larger value of χ required to model the fluctuations that occur at a microsecond time scale while resolving the remaining slow and fast time-scale oscillations of the OEO. The simulations also demonstrate a dependence of the evolution of the spikes with the strength of the stochastic component and the strength of the gain parameter. When the noise strength is increased, the spiking-bursting oscillations also increase which affects the slope of probability distribution of the spikes (ISI histogram), similarly to what is observed in other reported stochastically driven OEOs [35]. In respect to the gain, for a sufficient high gain condition, this will affect the OEO dynamics by suppressing the spiking-bursting oscillations before reaching a chaotic regime, similarly as reported in [20].

B. Synchronized Bursting

Bursting oscillations are typically generated as the evolution of the slow variables of a given system switches the fast dynamics between steady state and oscillatory dynamics. The burst firing is composed of burst of spikes with nearly regular short ISIs, interspersed with longer intrabrust intervals. Mechanisms of generating burst firing and related rich dynamics including chaos have been intensively studied from the viewpoint of biophysical and dynamical modeling of nerve membranes by introducing slow variables to fast spike dynamics [39]. One simple method to provide a synchronized bursting firing is to introduce into the system an additional periodic slow time scale that can synchronize the bursting signals. Since our OEO can be externally injected, Fig. 1, synchronization to external electrical signals is a simple and robust method to provide an additional slow variable.

We investigate the generation of synchronized burst firing by means of electrical injection of a control signal. Fig. 6(a)-(i) and (a)-(ii) shows a transition between unsynchronized and synchronized bursting of spikes employing a 55 MHz sinusoidal

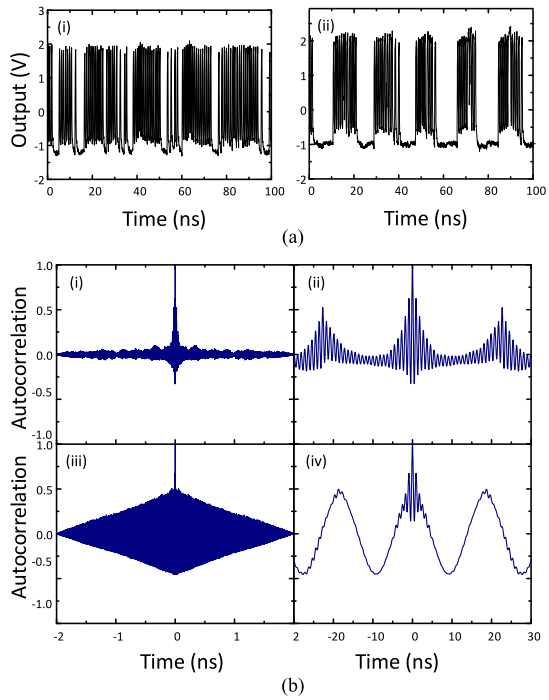

Fig. 6. (a) Unsynchronized (i) and synchronized (ii) bursting signals as a function of the amplitude of the periodic control signal (i) 250 mV, and (ii) 400 mV. (b) Corresponding autocorrelation plots as a function of the amplitude: unsynchronization (i) 250 mV and (ii) 250 mV (zoom-in); synchronization (iii) 400 mV; (iv) 400 mV (zoom-in).

electrical control signal. When the amplitude of the signal is increased above a certain value, a clear synchronized bursting is achieved with an intra-interval of ∼18 ns, while keeping the fast repetition of ∼0.8 ns of the inter-burst time scale. We observed that the intraburst interval could be controlled by tuning the frequency of the injected electrical control signal.

The ISI approach used previously to analyze the corresponding time series does not allow for an analysis of the synchronized bursting since the time series exhibits bunched spiking patterns and thus different timescales. Therefore, we consider the autocorrelation function as an alternative tool. This analysis measures the amount of periodicity in the autocorrelations, and thus the temporal regularity of the bursting activity. Fig. 6(b)-(i) shows the autocorrelation function of the unsynchronized bursts showing a week periodicity of the intra-burst slow timescale and strong inter-burst amplitude, Fig. 6(b)-(ii). However, when synchronized, Fig. 6(b)-(iii), the autocorrelation enables to distinguish between inter-burst and intra-burst timescales showing a strong periodicity of the intra-burst timescale, Fig. 6(b)-(iv).

The possibility to control the time repetition of the random spiking-bursting behavior presented here using external injection provides a robust and flexible method to tune the bursting behavior without requiring changes of the remaining characteristics of the OEO configuration.

IV. Conclusion

We have demonstrated a multiple timescale long-delayed OEO incorporating a broadband MFP, enabling the generation of ultrafast spiking and bursting oscillations. We have reported a scenario transition from spiking into bursting in a Neimark-Sacker type route to chaos, a secondary Hopf bifurcation which is a consequence of the long delay influence and that promotes the appearance of bursting activities in the OEO, depending on the gain and delay control parameters. The OEO exhibits typical response times of around 450 ps and pulse widths ∼250 ps. Also shown was the possibility to control the time repetition of the random spiking-bursting using external injection which provides a robust and flexible method to tune and control the longer intraburst intervals.

The spiking and bursting patterns reported here seem to be analogous to the role of local synaptic activity observed in large neuronal network dynamics with different coupling strengths. Since our OEO can operate at much higher speeds than the slow speed typically found in biological neurons, it has interest in a number of emerging photonics applications including neuromorphic information processing and reservoir computing tasks.

Considering that similar pattern formation has been found to regulate local synaptic activity observed in large neuronal networks, the investigation on the conditions that trigger the emergence of spiking phenomena in long delayed feedback systems provides a better understanding of processing of sensory information. These studies can shed a new light in similar phenomena that happens in nature at the physical, chemical, and biological level and that are critically involved in almost every cognitive complex tasks, including information coding and memory formation.

References

[1] C. A. Del Negro, C. G. Wilson, R. J. Butera, H. Rigatto, and J. C. Smith, "Periodicity, mixed-mode oscillations, and quasiperiodicity in a rhythm-generating neural network," *Biophys. J.*, vol. 82, no. 1, pp. 206–214, Jan. 2002.

[2] V. Petrov, S. K. Scott, and K. Showalter, "Mixed-mode oscillations in chemical systems," *J. Chem. Phys.*, vol. 97, no. 9, pp. 6191–6198, Nov. 1992.

[3] A. M. Yacomotti, M. C. Eguia, J. Aliaga, O. E. Martinez, G. B. Mindlin, and A. Lipsich, "Interspike time distribution in noise driven excitable systems," *Phys. Rev. Lett.*, vol. 83, no. 2, pp. 292–295, Jul. 1999.

[4] S. Barland, O. Piro, M. Giudici, J. R. Tredicce, and S. Balle, "Experimental evidence of van der Pol–Fitzhugh–Nagumo dynamics in semiconductor optical amplifiers," *Phys. Rev. E*, vol. 68, no. 3, p. 036209, Sep. 2003.

[5] M. Giudici, C. Green, G. Giacomelli, U. Nespolo, and J. R. Tredicce, "Andronov bifurcation and excitability in semiconductor lasers with optical feedback," *Phys. Rev. E*, vol. 55, no. 6, pp. 6414–6418, Jun. 1997.

[6] J. Ohtsubo, *Semiconductor Lasers: Stability, Instability and Chaos*. London, U.K.: Springer, 2005.

[7] A. S. Samardak, A. Nogaret, N. B. Janson, A. Balanov, I. Farrer, and D. A. Ritchie, "Spiking computation and stochastic amplification in a neuron-like semiconductor microstructure," *J. Appl. Phys.*, vol. 109, no. 10, p. 102408, May 2011.

[8] S. Barbay, R. Kuszelewicz, and A. M. Yacomotti, "Excitability in a semiconductor laser with saturable absorber," *Opt. Lett.*, vol. 36, no. 23, pp. 4476- 4478, Nov. 2011.

[9] B. J. Shastri, M. A. Nahmias, A. N. Tait, Y. Tian, B. Wu, and P. R. Prucnal, "Graphene excitable laser for photonic spike processing," in *Proc. IEEE Photon. Conf.*, Sep. 2013, pp. 1–2.

[10] X. Y. Yao and L. Maleki, "Optoelectronic oscillator for photonic systems," *IEEE J. Quantum Electron.*, vol. 32, no. 7, pp. 1141–1149, Jul. 1996.

[11] L. Maleki, D. Eliyahu, and A. B. Matsko, "Optoelectronic oscillator," in *Broadband Optical Modulators: Science, Technology, and Applications*,

A. Chen and E. Murphy, Eds. Boca Raton, FL, USA: CRC Press, 2011, pp. 467–488.
[12] X. S. Yao and L. Maleki, "Multiloop optoelectronic oscillator," *IEEE J. Quantum Electron.*, vol. 36, no. 1, pp. 79–84, Jan. 2000.
[13] B. Romeira, J. Javaloyes, J. M. L. Figueiredo, C. N. Ironside, H. I. Cantu, and A. E. Kelly, "Delayed feedback dynamics of Liénard-type resonant tunneling-photo-detector optoelectronic oscillators," *IEEE J. Quantum Electron.*, vol. 49, no. 1, pp. 31–42, Jan. 2013.
[14] N. Yu, E. Salik, and L. Maleki, "Ultralow-noise mode-locked laser with coupled optoelectronic oscillator configuration," *Opt. Lett.*, vol. 30, no. 10, pp. 1231–1233, Nov. 2005.
[15] Y. K. Chembo, A. Hmima, P. Lacourt, L. Larger, and J. M. Dudley, "Generation of ultralow jitter optical pulses using optoelectronic oscillators with time-lens soliton-assisted compression," *J. Lightw. Technol.*, vol. 27, no. 22, pp. 5160–5167, Nov. 2009.
[16] J. Lasri, A. Bilenca, D. Dahan, V. Sidorov, G. Eisenstein, D. Ritter, and K. Yvind, "Self-starting hybrid optoelectronic oscillator generating ultra low jitter 10-GHz optical pulses and low phase noise electrical signals," *IEEE Photon. Technol. Lett.*, vol. 14, no. 7, pp. 1004–1006, Jul. 2002.
[17] J. Lasri, P. Devgan, R. Tang, and P. Kumar, "Self-starting optoelectronic oscillator for generating ultra-low-jitter high-rate (10 GHz or higher) optical pulses," *Opt. Exp.*, vol. 11, no. 12, pp. 1430–1435, Jun. 2003.
[18] A. Sherman and M. Horowitz, "Ultralow-repetition-rate pulses with ultralow jitter generated by passive mode-locking of an optoelectronic oscillator," *J. Opt. Soc. Amer. B*, vol. 30, no. 11, pp. 2980–2983, Nov. 2013.
[19] K. E. Callan, L. Illing, Z. Gao, D. J. Gauthier, and E. Scholl, "Broadband chaos generated by an optoelectronic oscillator," *Phys. Rev. Lett.*, vol. 104, no. 11, p. 113901, Mar. 2010.
[20] B. Romeira, F. Kong, W. Li, J. M. L. Figueiredo, J. Javaloyes, and J. Yao, "Broadband chaotic signals and breather oscillations in an optoelectronic oscillator incorporating a microwave photonic filter," *J. Lightw. Technol.*, vol. 32, no. 20, pp. 3933–3941, Oct. 2014.
[21] M. Peil, M. Jacquot, Y. K. Chembo, L. Larger, and T. Erneux, "Routes to chaos and multiple time scale dynamics in broadband bandpass nonlinear delay electro-optic oscillators," *Phys. Rev. E*, vol. 79, no. 2, p. 026208, Feb. 2009.
[22] D. P. Rosin, K. E. Callan, D. J. Gauthier, and E. Schöll, "Pulse-train solutions and excitability in an optoelectronic oscillator," *Europhys. Lett.*, vol. 96, no. 3, pp. 34001 (6 pp.), Nov. 2011.
[23] T. R. Chay and J. Rinzel, "Bursting, beating, and chaos in an excitable membrane model," *Biophys. J.*, vol. 47, no. 3, pp. 357–366, Mar. 1985.
[24] W. Bao and J.-Y. Wu, "Propagating wave and irregular dynamics: Spatiotemporal patterns of cholinergic theta oscillations in neocortex in vitro," *J. Neurophysiol.*, vol. 90, no. 1, pp. 333–341, Feb. 2003.
[25] K. Ikeda and K. Matsumoto, "High-dimensional chaotic behavior in systems with time-delay feedback," *Phys. D*, vol. 29, nos. 1/2, pp. 223–235, Nov./Dec. 1987.
[26] C. W. Gardiner, *Handbook of Stochastic Methods*. H. Haken Ed. Berlin, Germany: Springer-Verlag, 1985.
[27] E. C. Levy, M. Horowitz, and C. R. Menyuk, "Modeling optoelectronic oscillators," *J. Opt. Soc. Amer. B*, vol. 26, no. 1, pp. 148–159, Jan. 2009.
[28] D. Lyons, E. Horjales-Araujo, and C. Broberger, "Synchronized network oscillations in rat tuberoinfundibular dopamine neurons: Switch to tonic discharge by thyrotropin-releasing hormone," *Neuron*, vol. 65, no. 2, pp. 217–229, Jan. 2010.
[29] K. Tsaneva-Atanasova, A. Sherman, F. Van Goor, and S. S. Stojilkovic, "Mechanism of spontaneous and receptor-controlled electrical activity in pituitary somatotrophs: Experiments and theory," *J. Neurophysiol.*, vol. 98, no. 1, pp. 131–144, May 2007.
[30] J. Tabak, M. Tomaiuolo, A. Gonzalez-Iglesias, L. Milescu, and R. Bertram, "Fast-activating voltage-and calcium-dependent potassium BK conductance promotes bursting in pituitary cells: A dynamic clamp study," *J. Neurosci.*, vol. 31, no. 46, pp. 16855–16863, Nov. 2011.
[31] T. Vo, R. Bertram, J. Tabak, and M. Wechselberger, "Mixed mode oscillations as a mechanism for pseudo-plateau bursting," *J. Comput. Neurosci.*, vol. 28, no. 3, pp. 443–458, Jun. 2010.
[32] W. Teka, J. Tabak, T. Vo, M. Wechselberger, and R. Bertram, "The dynamics underlying pseudo-plateau bursting in a pituitary cell model," *J. Math. Neurosci.*, vol. 1, no. 12, pp. 1–12, Nov. 2011.
[33] J. Rinzel, "A formal classification of bursting mechanisms in excitable systems," in *Mathematical Topics in Population Biology, Morphogenesis, and Neurosciences, Lecture Notes in Biomathematics*, E. Teramoto and M. Yamaguti, Eds. Berlin, Germany: Springer, 1987, pp. 267–281.
[34] B. M. A. Nahmias, B. J. Shastri, A. N. Tait, and P. R. Prucnal, "A leaky integrate-and-fire laser neuron for ultrafast cognitive computing," *IEEE J. Sel. Topics Quantum Electron.*, vol. 19, no. 5, pp. 1800212, Sep./Oct. 2013.
[35] B. Romeira, J. Javaloyes, C. N. Ironside, J. M. L. Figueiredo, S. Balle, and O. Piro, "Excitability and optical pulse generation in semiconductor lasers driven by resonant tunneling diode photo-detectors," *Opt. Exp.*, vol. 21, no. 18, pp. 20931–20940, Sep. 2013.
[36] R. Lavrov, M. Peil, M. Jacquot, L. Larger, V. Udaltsov, and J. Dudley, "Electro-optic delay oscillator with nonlocal nonlinearity: Optical phase dynamics, chaos, and synchronization," *Phys. Rev. E*, vol. 80, no. 2, p. 026207, Aug. 2009.
[37] E. M. Izhikevich, "Neural excitability, spiking and bursting," *Int. J. Bifurcation Chaos*, vol. 10, no. 6, pp. 1171–1266, Jun. 2000.
[38] G. Tanaka, M. A. F. Sanjuán, and K. Aihara, "Crisis-induced intermittency in two coupled chaotic maps: Towards understanding chaotic itinerancy," *Phys. Rev. E*, vol. 71, no. 1, p. 016219, Jan. 2005.
[39] W. Teka, J. Tabak, and R. Bertram, "The relationship between two fast/slow analysis techniques for bursting oscillations," *Chaos*, vol. 22, no. 4, pp. 043117 (10 pp.), Nov. 2012.

Bruno Romeira (M'13) received the five-year Diploma degree in physics and chemistry from the University of the Algarve, Faro, Portugal, in 2006, and the Ph.D. degree in physics (summa cum laude) and the title of European Ph.D. from the same university, jointly with the University of Glasgow, Glasgow, U.K., and the University of Seville, Seville, Spain, in 2012.

He is currently involved in a Postdoctoral Fellowship Program at the Department of Physics, Center of Electronics Optoelectronics and Telecommunications, University of the Algarve, and at the Microwave Photonics Research Laboratory, University of Ottawa, Ottawa, ON, Canada, as a Visiting Postdoctoral Researcher. His research interests include disciplines in applied physics and engineering, which include semiconductor physics, solid-state electronics, and optoelectronics. He is also interested in complex systems, chaos, and synchronization for novel applications in information and communication technologies.

Dr. Romeira received the "Young Researchers Incentive Programme" Award from the Calouste Gulbenkian Foundation, Portugal, in 2009, and the "IEEE Photonics Society Graduate Student Fellowship" from the IEEE Photonics Society, USA, in 2011. His Ph.D. thesis entitled "Dynamics of Resonant Tunneling Diode Optoelectronic Oscillators" received the "Best Ph.D. Thesis in Optics and Photonics in Portugal in 2012" by the Portuguese Society of Optics and Photonics (SPOF).

Fanqi Kong (S'13) received the B.Eng. degree in optoelectronics information engineering from the Huazhong University of Science and Technology, Wuhan, China, in 2012. He is currently working toward the M.A.Sc. degree with the School of Electrical Engineering and Computer Science, University of Ottawa, Ottawa, ON, Canada.

His current research interests include photonic generation of microwave signals and applications in sensing systems.

José M. L. Figueiredo (M'09) received the B.Sc. degree in physics (optics and electronics) and the M.Sc. degree in optoelectronics and lasers from the University of Porto, Porto, Portugal, in 1991 and 1997, respectively. He received the Ph.D. degree in physics from the University of Porto in "co-tutela" with the University of Glasgow, Glasgow, U.K., in 2000.

He worked with the University of Glasgow on the optoelectronic properties of resonant tunneling diodes. In 1999, he joined the Department of Physics, University of the Algarve, Faro, Portugal. His current research interests include resonant tunneling diode microwave and millimeter-wave oscillators, the generation of microwave-photonic signals, generation of chaotic signals, and terahertz communications.

Julien Javaloyes (M'11) was born in Antibes, France. He received the M.Sc. degree in physics from the École Normale Supérieure de Lyon, Lyon, France, and the Ph.D. degree in physics from the Institut Non Linéaire de Nice, Université de Nice Sophia Antipolis, Nice, France, where he studied the recoil induced instabilities and self-organization processes occurring in cold atoms.

He worked on delay induced dynamics in coupled semiconductor lasers during a postdoctoral stage in Brussels, and on VCSEL polarization dynamics in Palma de Mallorca. He was a Research Associate with Glasgow University, Glasgow, U.K., where provided for the modeling of the dynamics of monolithic semiconductor diodes. He joined the Physics Department, Universitat de les Illes Balears, Palma, Spain, in 2010, as a Ramón y Cajal Fellow. His current research interests include laser dynamics, atom-light interaction modeling and applied numerical bifurcation analysis.

Jianping Yao (M'99–SM'01–F'12) received the Ph.D. degree in electrical engineering from the Université de Toulon, Toulon, France, in December 1997.

He joined the School of Electrical and Electronic Engineering, Nanyang Technological University, Singapore, as an Assistant Professor in 1998. In December 2001, he joined the School of Electrical Engineering and Computer Science, University of Ottawa, as an Assistant Professor, where he became a tenured Associate Professor in 2003, and a Full Professor in 2006. He was appointed as the University Research Chair in Microwave Photonics in 2007. From July 2007 to June 2010, he was the Director of the Ottawa-Carleton Institute for Electrical and Computer Engineering. He was reappointed as the Director of the Ottawa-Carleton Institute for Electrical and Computer Engineering in 2013. He is currently a Professor and University Research Chair at the School of Electrical Engineering and Computer Science, University of Ottawa, Ottawa, ON, Canada. He has published more than 450 papers, including more than 260 papers in peer-reviewed journals and 190 papers in conference proceedings. He was a Guest Editor for the Focus Issue on Microwave Photonics in Optics Express in 2013 and a Feature Issue on Microwave Photonics in *Photonics Research* in 2014. He is currently a Topical Editor for *Optics Letters*, and serves on the Editorial Board of the IEEE TRANSACTIONS ON MICROWAVE THEORY AND TECHNIQUES, *Optics Communications*, and *Science Bulletin*. He is the Chair of numerous international conferences, symposia, and workshops, including the Vice-TPC Chair of the 2007 IEEE Microwave Photonics Conference, TPC Cochair of the 2009, and 2010 Asia-Pacific Microwave Photonics Conferences, TPC Chair of the high-speed and broadband wireless technologies subcommittee of the 2009–2012 IEEE Radio Wireless Symposia, TPC Chair of the microwave photonics subcommittee of the 2009 IEEE Photonics Society Annual Meeting, TPC Chair of the 2010 IEEE Microwave Photonics Conference, and General Cochair of the 2011 IEEE Microwave Photonics Conference.

Dr. Yao received the International Creative Research Award at the University of Ottawa in 2005. He also received the George S. Glinski Award for Excellence in Research in 2007. He was selected to receive an inaugural OSA outstanding reviewer award in 2012. He is an IEEE MTT-S Distinguished Microwave Lecturer for 2013 to 2015. He is a Registered Professional Engineer of Ontario. He is a Fellow of the Optical Society of America and the Canadian Academy of Engineering.